Electronical Supporting Information

Thermo- and oxidation-sensitive poly(meth)acrylates

based on alkyl sulfoxides:

Dual-responsive homopolymers from one functional group

Doğuş Işık,[1] Elisa Quaas,[2] Daniel Klinger[1]*

[1] *Institute of Pharmacy, Freie Universität Berlin, Königin-Luise-Straße 2-4, 14195 Berlin, Germany*
[2] *Institute of Chemistry, Freie Universität Berlin, Takustraße 3, 14195 Berlin, Germany*
*E-mail: daniel.klinger@fu-berlin.de

Content

I. Preparation of alkyl sulfoxide (meth)acrylate monomers

To realize the anticipated sulfoxide polymer library, functional alkyl sulfoxide (meth)acrylate monomers were synthesized via a straight-forward two-step reaction route (**Fig. S1**).
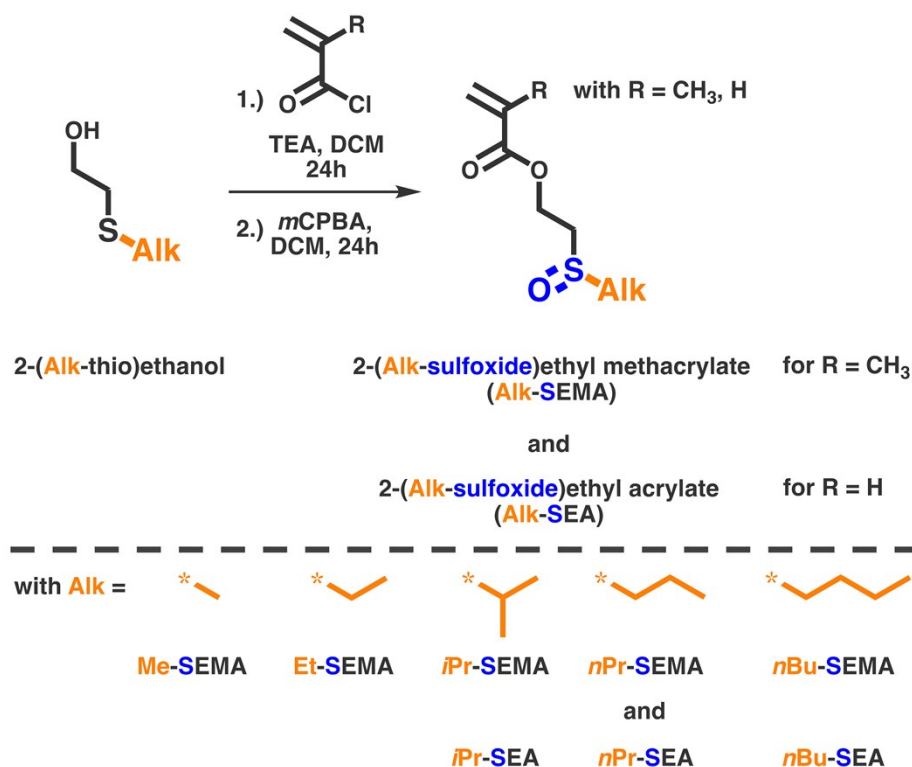
Fig. S1 Successful synthesis of a functional sulfoxide monomer library *via* a two-step reaction route. The monomers were denoted as follows: 2-(*Alkyl*-**s**ulfoxide)**e**thyl **m**eth**a**crylates (*Alkyl*-**SEMA**) with methyl (Me), ethyl (Et), *iso*propyl (*i*Pr), *n*-propyl (*n*Pr) and, *n*-butyl (*n*Bu) as alkyl groups and 2-(*Alkyl*-**s**ulfoxide)**e**thyl **a**crylates (*Alkyl*-**SEA**) with *iso*propyl (*i*Pr), *n*-propyl (*n*Pr), *n*-butyl (*n*Bu) as alkyl groups, respectively.

This facile, fast and efficient synthesis route affords the targeted sulfoxide (meth)acrylates as pure monomer reagents. This was examined by ^{1}H NMR spectroscopy (**Fig. S2**).
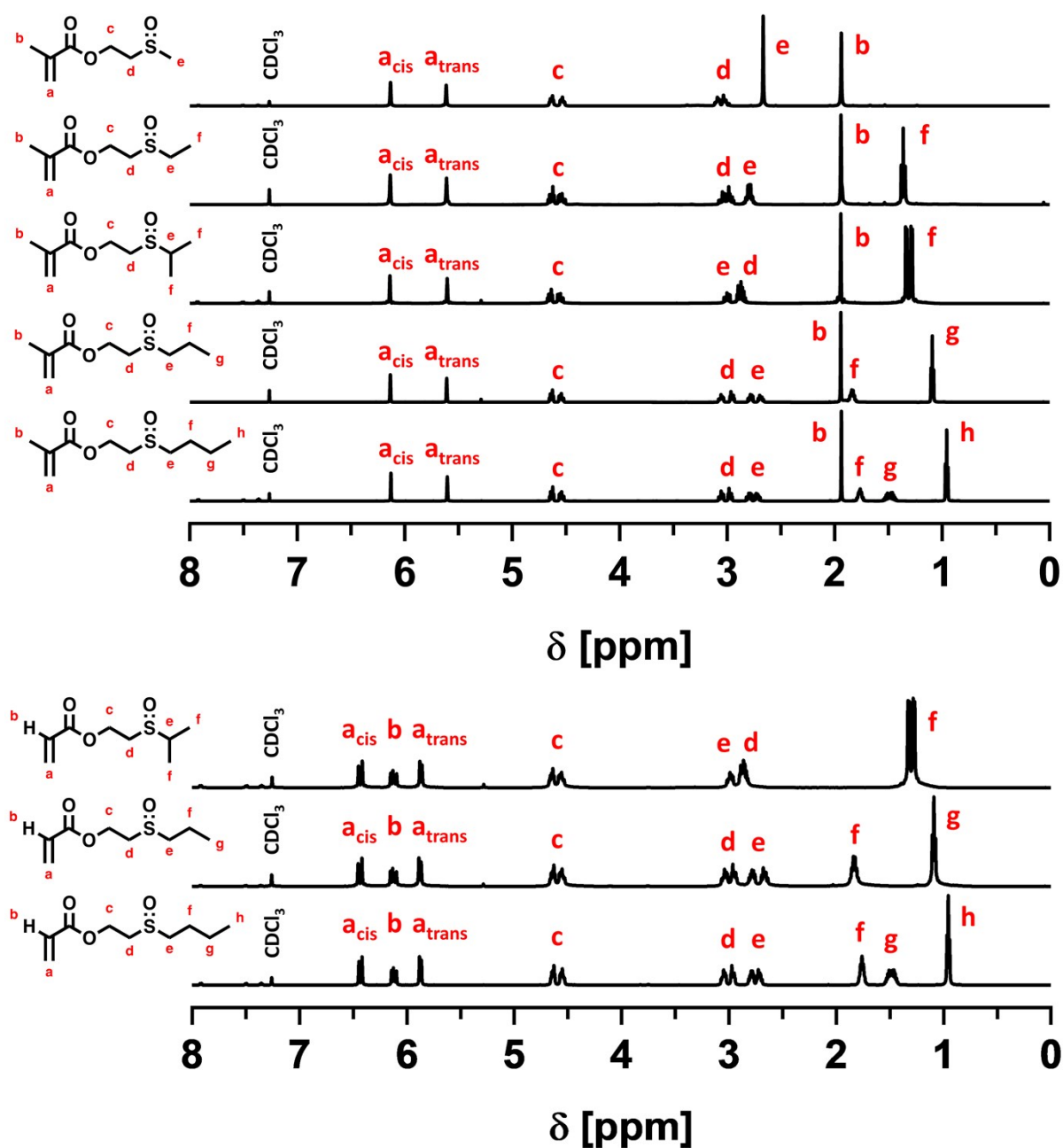

Fig. S2 ^{1}H NMR spectra of the sulfoxide (meth)acrylate monomers show pure monomer reagents were obtained *via* a straightforward two-step reaction route.

II. RAFT polymerization of acrylate monomers

The RAFT solution homopolymerization of the alkyl sulfoxide acrylate monomers was initially performed using the same reaction conditions as for the polymethacrylates - cumyl dithiobenzoate (CDTB) as a chain transfer agent (CTA), AIBN as a radical initiator, and DMF as solvent with an initial feed ratio of [Monomer]$_0$: [CDTB]$_0$: [AIBN]$_0$ = 150 : 1 : 0.125. However, under these conditions only small molecular weight polymers were obtained (**Table S1**). This stems from the lower conversions in comparison to the poly*meth*acrylates thus indicating a slower polymerization process.

Table S1 RAFT homopolymerisation of acrylate monomers *i*Pr-SEA, *n*Pr-SEA and *n*Bu-SEA. Reaction were performed in DMF ([M] = 1 M) with [M] : [CDTB] : [I] = 150 : 1 : 0.125 at 75 °C for a reaction time of 24 h.

Polymer	[M]/[CTA]	Conv.^{a} (%)	$M_{n,target}$ (g mol^{-1})	$M_{n,NMR}$ (g mol^{-1})	DP	$M_n{}^b{}_{,GPC}$ (g mol^{-1})	$Đ^b$
P(*n*Pr-SEA)	150	61	28 540	17 400	87	10 500	1.24
P(*i*Pr-SEA)	150	58	28 540	16 500	91	11 400	1.25
P(*n*Bu-SEA)	150	60	30 640	18 300	90	10 100	1.24

^{a} Conversion measured by ^{1}H NMR spectroscopy. ^{b} DMF LiBr (10 mM) eluent, linear PMMA standard.

To prepare polyacrylates with higher molecular weights, briefly, BBDT in dioxane was used with an initial [M]/[CTA] = 250 to account for the slow polymerization and the corresponding low conversion. Under these polymerization conditions, polyacrylates with degrees of polymerization comparable to the poly*meth*acrylates with [M]/[CTA] = 150 were obtained with reasonable polydispersities (Manuscript, **Table 1**).

III. Determination of polymer molecular weight (M$_{n,NMR}$) by ^{1}H NMR spectroscopy

The molecular weights of the presented RAFT polymers were calculated with the help of ^{1}H NMR spectroscopy by end group analysis. For this, the end group integrals (chain transfer agent) were compared to the integral of the monomeric units (**Fig. S3**). Exemplary the molecular weight (M$_{n,NMR}$) calculation for P(iPr-SEA)$_{127}$ is shown as follows:

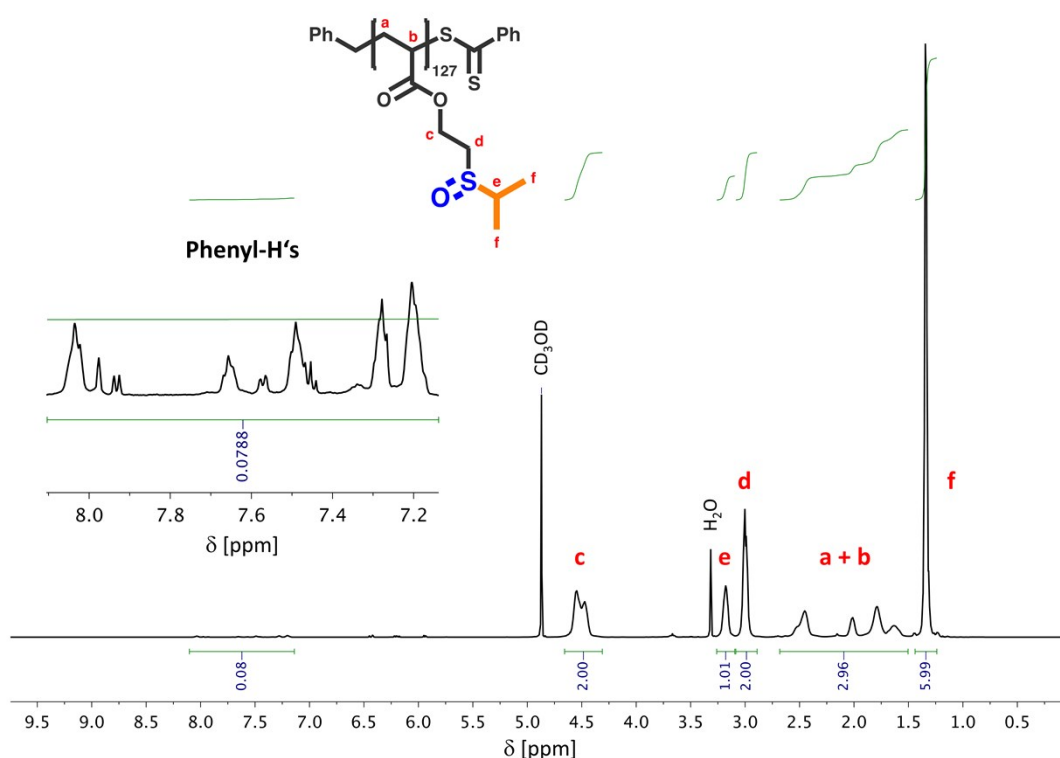**Fig. S3** ^{1}H NMR spectrum of P(iPr-SEA)$_{127}$ for the determination of the degree of polymerization (DP)

First, the end group protons (chain transfer agent) were identified at 8.0 – 7.2 ppm (**Fig. S3**, Phenyl-***H***'s). From these phenyl protons the integral value per end group proton was calculated. This value was set in relation to the integral value for one -OC***H***$_2$- proton (**c**) of the monomer to give the degree of polymerization.

Accordingly, the molecular weights of all RAFT polymers were calculated as shown above.

IV. Preparation of sulfone polymers

The hydrophobic sulfone polymers act as the control group for the assessment of the special thermo- and oxidation-responsive properties of the sulfoxide polymers. Therefore, a respective sulfone polymer library was investigated (**Fig. S4a**). The preparation of this polymer library was realized *via* a simple oxidation step using *meta*-chloroperbenzoic acid (*m*CPBA) (**Fig. S4b**).
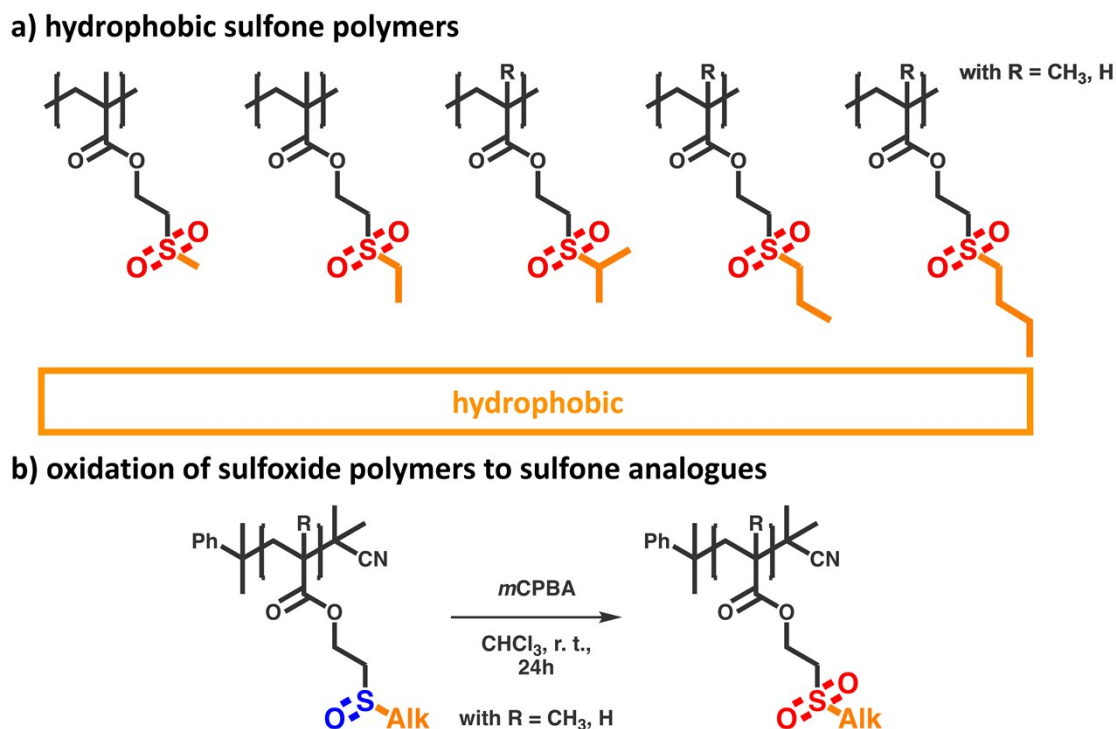

Fig. S4 a) Investigated library of hydrophobic sulfone (meth)acrylate polymers. Due to the overall hydrophobic nature of the alkyl sulfone structure, the sulfone poly(meth)acrylates represent the control group to the amphiphilic sulfoxide polymers in terms of tunable thermo-responsive polymer properties and the quantitative oxidation response. **b)** The synthesis was successfully achieved via the oxidation of the functional sulfoxide moieties.

The presented synthetic strategy also benefits from the prior end group removal (**Fig. S4b**) since the direct oxidation of the RAFT end group could either give reactive sulfines that readily decompose to thioesters and elemental sulfur[1] or hydroperoxide end groups that could subsequently be reduced to hydroxyl groups.[2, 3] These side reactions show that a more inert end group is desired in the sulfoxide to sulfone oxidation process.

The synthesized sulfone polymethacrylate library was found to exhibit similar molecular weights and polymer dispersities with respect to its sulfoxide analogues (**Table S2**). This ensures comparability between both respective polymer libraries.

Table S2 A complementary library of sulfone *meth*acrylate polymers was prepared by simple oxidation of the previously prepared sulfoxide polymers ensuring comparability (similar DP and Đ) between both polymer libraries.

Polymer	$M_{n,target}$ (g mol^{-1})	$M_{n,NMR}$ (g mol^{-1})	DP	$M_n{}^b{}_{,GPC}$ (g mol^{-1})	$Đ^b$
P(Me-SO$_2$EMA)	28 810	24 200	126	24 400	1.28
P(Et-SO$_2$EMA)	30 940	28 300	137	25 500	1.28
P(*i*Pr-SO$_2$EMA)	33 040	29 100	132	24 600	1.28
P(*n*Pr-SO$_2$EMA)	33 040	28 900	131	25 800	1.26
P(*n*Bu-SO$_2$EMA)	35 150	32 800	140	25 900	1.27
P(*n*Pr-SO$_2$EA)	30 940	16 300	79	13 900	1.23
P(*i*Pr-SO$_2$EA)	30 940	17 900	87	14 200	1.27
P(*n*Bu-SO$_2$EA)	33 040	18 500	84	13 400	1.23

[a] DMF LiBr (10 mM) eluent, linear PMMA standard.

As an example, this comparability was shown for the GPC traces of P(*i*Pr-SEMA) and P(*n*Pr-SEMA) and their respective sulfone analogues P(*i*Pr-SO$_2$EMA) and P(*n*Pr-SO$_2$EMA) (**Fig S5a** for P(*i*Pr-SEMA) vs. P(*i*Pr-SO$_2$EMA) and **Fig. S5b** for P(*n*Pr-SEMA) vs. P(*n*Pr-SO$_2$EMA)). The shape of the GPC peak and the elution time indicate that both polymer pairs exhibit comparable polymer structures.
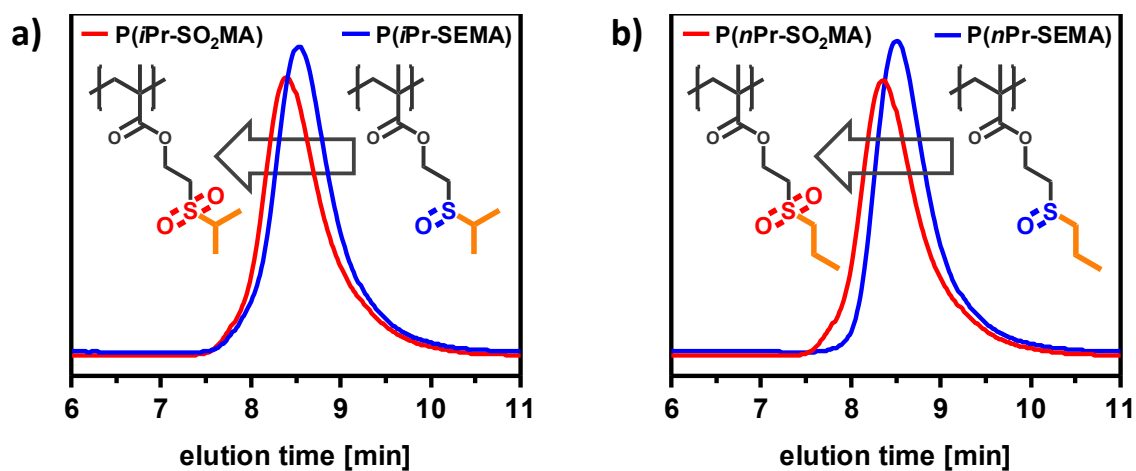
Fig. S5 Exemplary comparison between GPC traces of (**a**) P(*i*Pr-SEMA) and (**b**) P(*n*Pr-SEMA) and their respective oxidized sulfone analogues (**a**) P(*i*Pr-SO$_2$EMA) and (**b**) P(*n*Pr-SO$_2$EMA). The similarity of both respective GPC peaks and the comparable elution times indicate that both sulfoxide and sulfone polymer pairs exhibit similar molecular weights and polymer dispersities.

V. Assessment of thermo-responsive polymer properties

The temperature-dependent solution properties of P(nBu-SEMA)$_{119}$, P(nPr-SEMA)$_{130}$, P(iPr-SEMA)$_{128}$ and P(nPr-SEA)$_{124}$ were assessed via temperature-dependent (5 – 90 °C) optical transmission measurements. From these measurements, the observed cloud point temperatures (T_{cp}) were calculated through the minimum of the first derivative (inflection point) of the respective curves (**Fig. S6**). This approach represents a robust method to assess thermo-responsive polymer properties.[4]
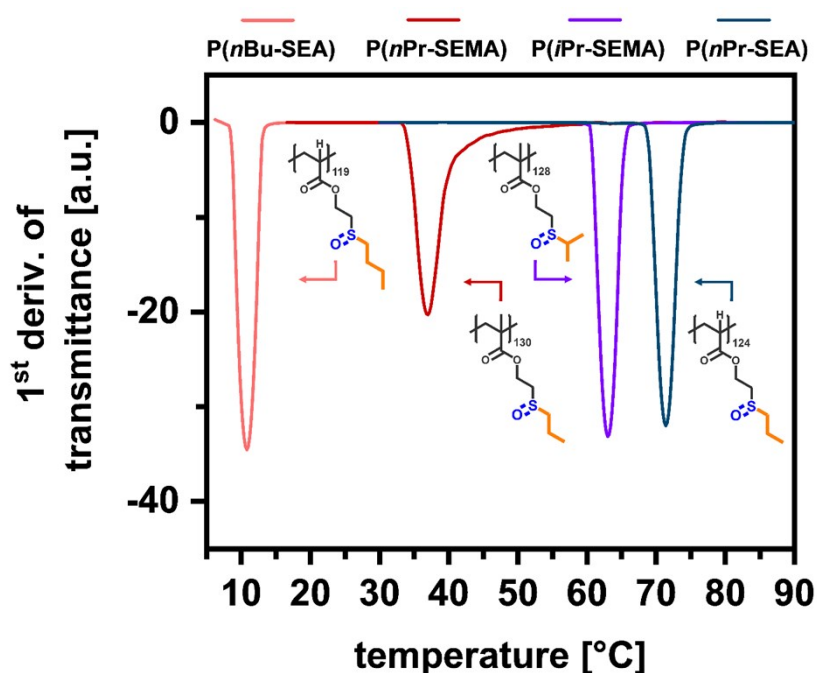

Fig. S6 Assessment of the cloud point temperature (T_{cp}'s) of P(nBu-SEMA)$_{119}$, P(nPr-SEMA)$_{130}$, P(iPr-SEMA)$_{128}$ and P(nPr-SEA)$_{124}$ *via* temperature-dependent (5 – 90 °C) optical transmission measurements. The T_{cp} represents the temperature at the inflection point of the normalized transmittance versus temperature curve.

VI. Control over DP via RAFT polymerization

To examine the influence of polymer molecular weight, i.e. degree of polymerization (DP), additional polymers of varying chain lengths of P(*i*Pr-SEMA) and P(*n*Pr-SEMA) were synthesized (**Table S3**). The DP was determined by end group analysis via ^{1}H NMR spectroscopy as a more accurate measure compared to the SEC analysis. Since SEC analysis is a relative method in which the size of a polymer is correlated to a certain standard, the polymer sizes can differ strongly depending on the used standard. For example, if PMMA is used, the higher molecular weight polymers were underestimated while with a PS standard, this trend is reversed and the smaller polymer are overestimated (Table S3). To circumvent this, NMR analysis was used to compare the DP of the polymers and their subsequent cloud points. The performed RAFT polymerization presents good control over the degree of polymerization DP and polymer dispersity.

Table S3 RAFT homopolymerisation shows good control over DP and dispersity of methacrylate monomers *i*Pr-SEMA and *n*Pr-SEMA. Reactions were performed in DMF ([M] = 1 M) with [M] : [CTA] : [I] = 250, 150, 50 : 1 : 0.125 at 75 °C for a reaction time of 24 h.

Polymer	[M]/ [CTA]	Conv.[a] (%)	$M_{n,target}$ (g mol^{-1})	$M_{n,NMR}$ (g mol^{-1})	DP	$M_n{}^{b}{}_{,GPC}$ w.r.t. PMMA (g mol^{-1})	$Đ^b$	$M_n{}^{c}{}_{,GPC}$ w.r.t. PS (g mol^{-1})	$Đ^c$
P(*i*Pr-SEMA)	250	85	51 070	43 500	209	29 300	1.29	44 600	1.21
	150	86	30 640	26 500	128	23 200	1.20	35 700	1.15
	50	99	10 210	10 100	48	11 000	1.23	19 000	1.15
P(*n*Pr-SEMA)	250	85	51 070	43 500	213	29 000	1.25	43 800	1.18
	150	88	30 640	26 900	130	22 400	1.21	34 700	1.16
	50	90	10 210	9 200	45	10100	1.24	17 800	1.15

[a] Conversion measured by ^{1}H NMR spectroscopy. [b] DMF LiBr (10 mM) eluent, linear PMMA standard. [c] DMF LiBr (10 mM) eluent, linear PS standard.

VII. Thermo-responsive properties of P(*n*Pr-SEMA) and P(*i*Pr-SEMA) free radical homopolymers

The effect of polymer molecular weight heterogeneity on the thermo-responsive properties was determined by investigating free radical homopolymers P(*n*Pr-SEMA) and P(*i*Pr-SEMA) with comparable molecular weight to their RAFT analogues. The resulting transmittance versus temperature curves for P(*n*Pr-SEMA) and P(*i*Pr-SEMA) are shown in **Fig. S7** and **Fig. S8**, respectively.

In **Fig. S7a**, the transmittance versus temperature curves for the three different molecular weight RAFT polymers P(*n*Pr-SEMA) are shown. Here, the cloud point temperatures shift moderately from 43 °C to 31 °C by increasing the molecular weight from 10 100 g/mol to 29 000 g/mol with narrow dispersities (1.21 – 1.25). In stark contrast, the cloud point temperatures of the comparable free radical polymers (13 600 g/mol – 27 000 g/mol with dispersities of 4.06 – 4.33) are all observed at around 28 - 29 °C (**Fig. S7b**).

Similarly, the heating and cooling cycle for three different molecular weight RAFT polymers P(*i*Pr-SEMA) are shown in **Fig. S8a**. Here, the cloud point temperatures shift moderately from 71 °C to 60 °C by increasing the molecular weight from 11 000 g/mol to 29 300 g/mol with narrow dispersities ($Đ$ = 1.20 – 1.29). In stark contrast, the cloud point temperatures of the comparable free radical polymers (14 000 g/mol – 28 900 g/mol with dispersities of $Đ$ = 2.88 – 3.34) are all observed at around 55 - 57 °C (**Fig. S8b**).

Additionally, no pronounced hysteresis is observed for both the P(*n*Pr-SEMA) and P(*i*Pr-SEMA) free radical homopolymers as well (**Fig. S7c-f** and **Fig. S8c-f**).

As a consequence, it can be concluded that the defined RAFT polymers exhibit a moderate difference in the cloud point temperatures for the different M_n's. This is not observed for the respective free radical polymers. This is probably based on the fact that the difference between a molecular weight of 14 000 g/mol – 28 900 g/mol is not as significant for dispersities of $Đ$ = 2.88 – 3.34 compared to dispersities of around $Đ$ = 1.2. Thus, the RAFT process allows also the T_{cp} to be tuned though the M_n.

Furthermore, in comparison to the RAFT polymers with similar M_n you can see that the free radical polymers always have a similar T_{cp}. The lower the M_n, the greater the effect. This means that the dispersity has a smaller influence on large polymers.
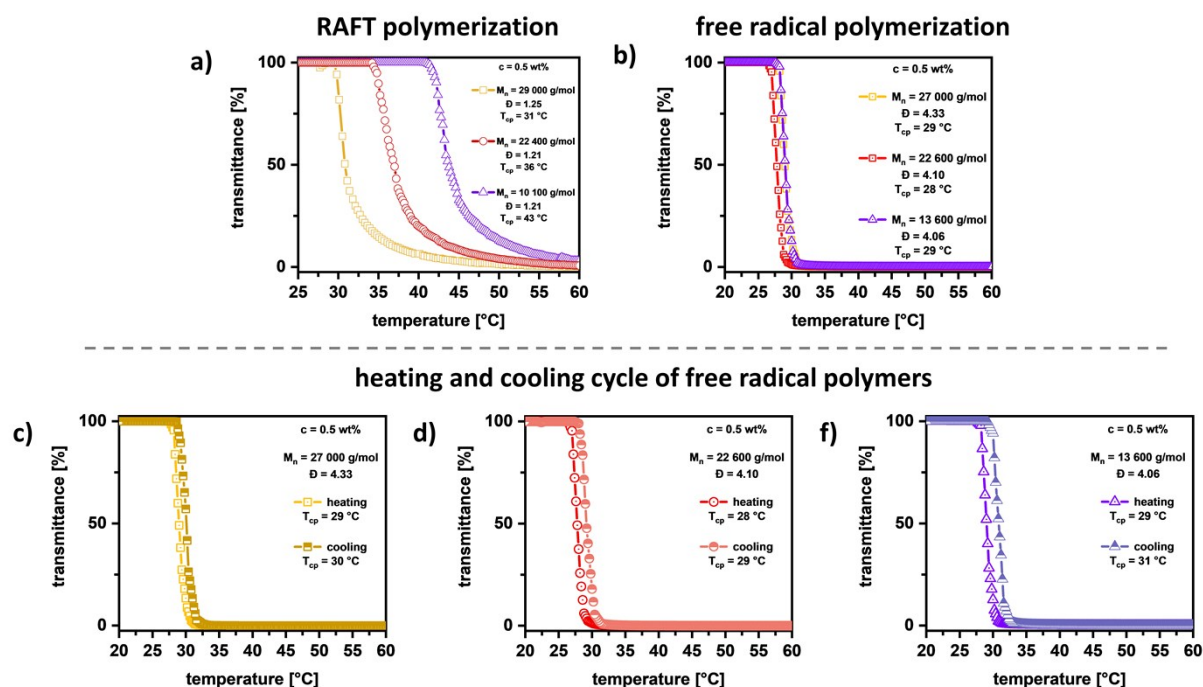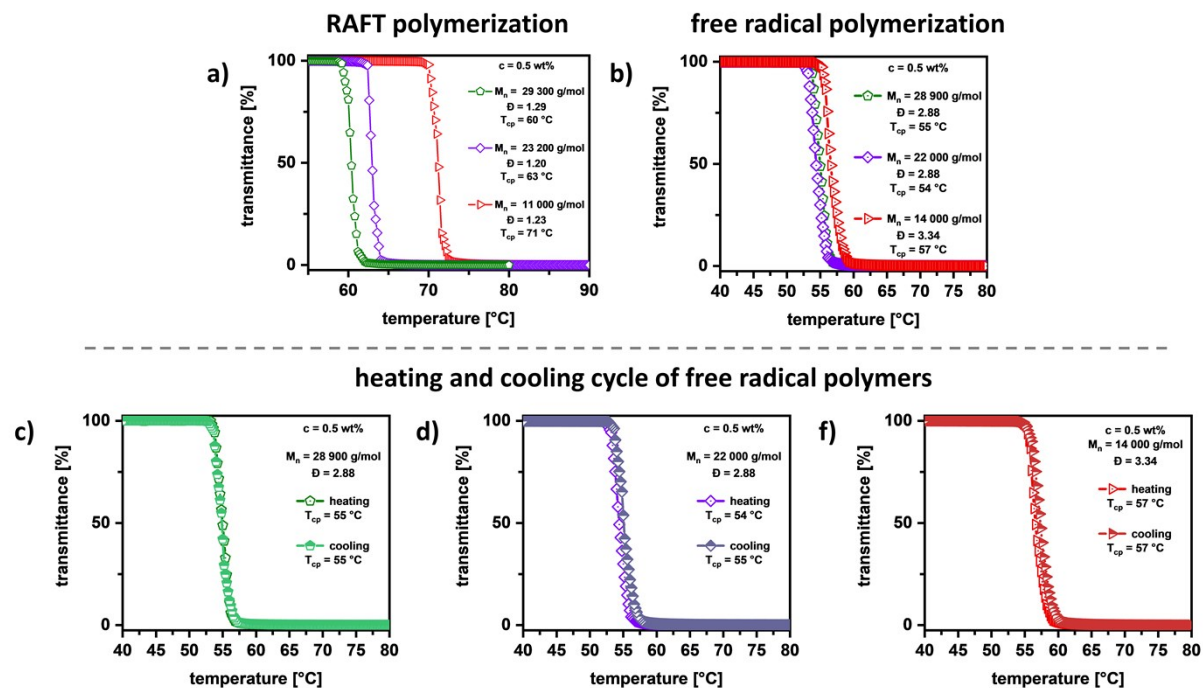
P(*n*Pr-SEMA)

Fig. S7 Transmittance versus temperature curves for the three different molecular weight P(*n*Pr-SEMA) by RAFT polymerization **(a)** and free radical homopolymers **(b)** with the respective heating and cooling cycle for the free radical polymer **(c-f)**.

P(*i*Pr-SEMA)

Fig. S8 Transmittance versus temperature curves for the three different molecular weight P(*i*Pr-SEMA) by RAFT polymerization **(a)** and free radical homopolymers **(b)** with the respective heating and cooling cycle for the free radical polymers **(c-f)**.

VIII. Hysteresis curves for P(*n*Pr-SEMA) and P(*i*Pr-SEMA)

The influence of heating and cooling on the temperature-dependent phase transition was assessed for P(*n*Pr-SEMA) and P(*i*Pr-SEMA). This measure is regarded to serve for the reversibility and robustness of the observed cloud point temperatures. The Figures **S9a** and **S9b** show the heating and cooling curves for P(*n*Pr-SEMA)$_{213}$ and P(*n*Pr-SEMA)$_{45}$ and the Figures **S9c** and **S9d** for P(*i*Pr-SEMA)$_{209}$ and P(*i*Pr-SEMA)$_{48}$, respectively. For all polymers these curves are nearly overlapping, thus not showing a pronounced hysteresis.
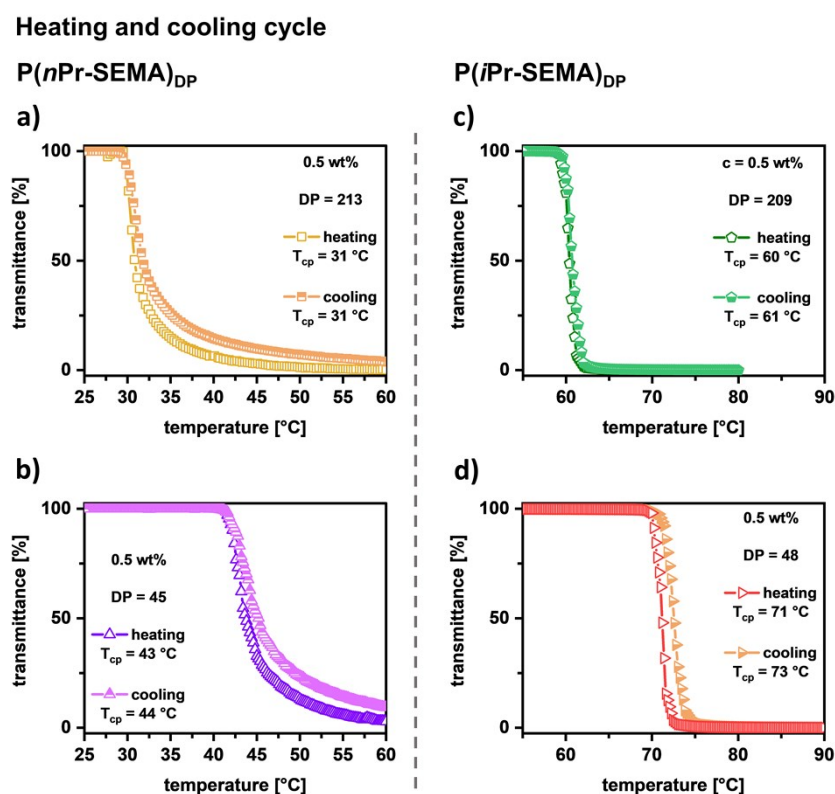

Fig. S9 Detailed temperature-responsive examinations on P(*n*Pr-SEMA) and P(*i*Pr-SEMA) in aqueous solution to study the effect of the heating or cooling cycle (hysteresis) **(a, b)** P(*n*Pr-SEMA)$_{213}$ and P(*n*Pr-SEMA)$_{45}$, **(c, d)** P(*i*Pr-SEMA)$_{209}$ and P(*i*Pr-SEMA)$_{48}$.

IX. Influence of the PBS on the cloud point temperature

The thermo-responsive polymer properties in phosphate buffered saline (PBS) solution as a biologically more relevant environment were analyzed. The respective temperature-dependent transmittance curves are shown in **Fig. S10a** for P(*n*Pr-SEMA) and **Fig. S10b** for P(*i*Pr-SEMA), respectively.
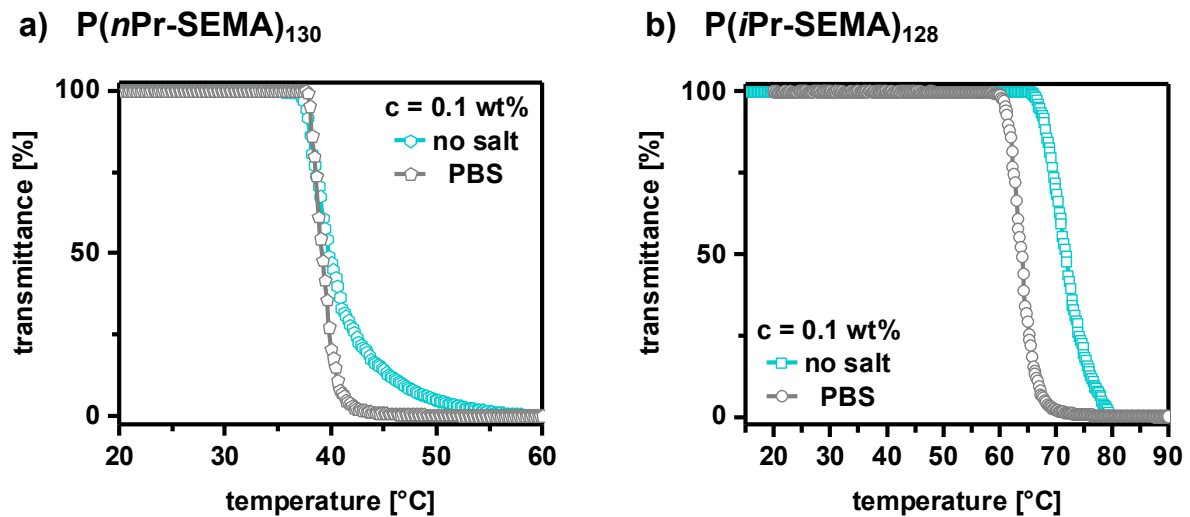

Fig. S10 Influence of PBS on the cloud point temperature of aqueous **(a)** P(*n*Pr-SEMA) and **(b)** P(*i*Pr-SEMA) solutions (0.1 wt%) showing the common observed "salting-out"-effect for thermo-responsive polymers.

X. ^{1}H-NMR investigations on the polymer oxidation reaction

The cloud point temperatures of P(nPr-SEMA)$_{130}$ and P(iPr-SEMA)$_{128}$ were expected to shift upon oxidation of the hydrophilic sulfoxide moieties to the respective hydrophobic sulfone groups. To investigate the oxidation reaction systematically the respective aqueous polymer solutions (0.1 wt%) were first subjected to different hydrogen peroxide concentrations (1.9 – 9.7 M) for 6 hours at 37 °C. ^{1}H-NMR spectroscopy was used to investigate the degree of oxidation (sulfone content) of the sulfoxides to sulfone side groups in the respective polymers (**Fig. S11** for P(nPr-SEMA)$_{130}$ and **Fig. S12** for P(iPr-SEMA)$_{130}$).
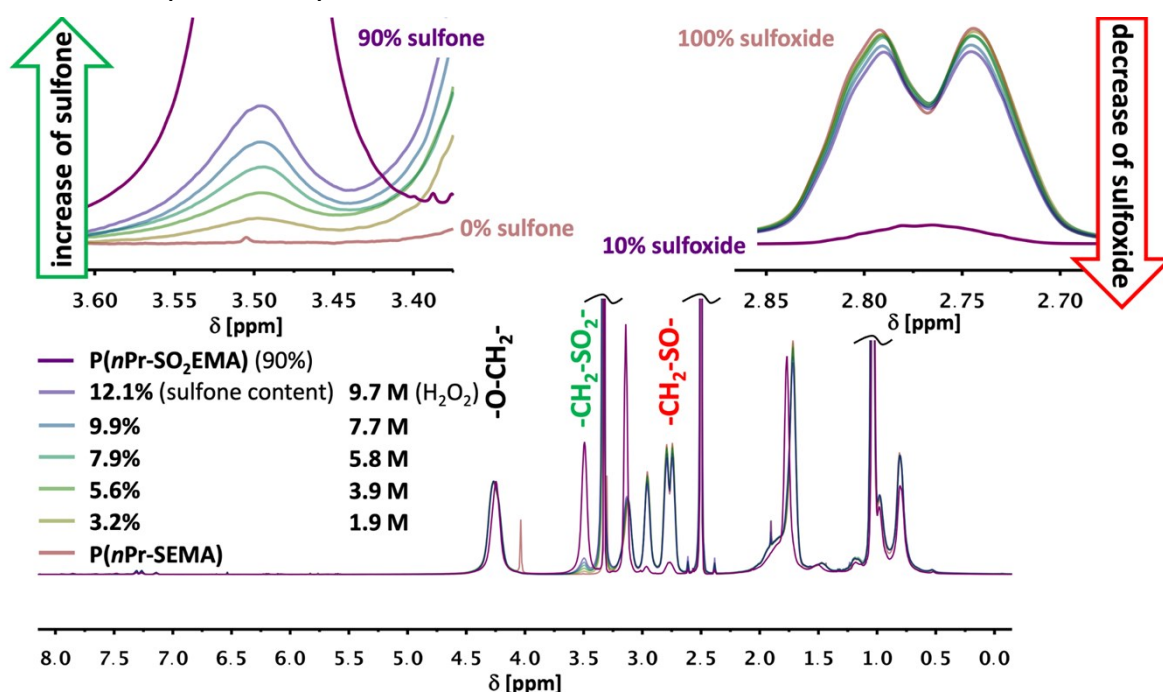
Oxidation of P(nPr-SEMA)$_{130}$

Fig. S11 ^{1}H-NMR investigation on the partial oxidation of P(nPr-SEMA)$_{130}$ after subjection to different H$_2$O$_2$ concentration (1.9 – 9.7 M) for 6 hours at 37 °C. Upon oxidation the aliphatic group next to the sulfoxide (-CH_2-SO-) at 2.77 ppm decreases gradually, while a new peak at 3.49 ppm appears which can be assigned to the sulfone (-CH_2-SO$_2$-). All spectra were normalized to the respective aliphatic group next to the methacrylate moiety (-O-CH_2-).
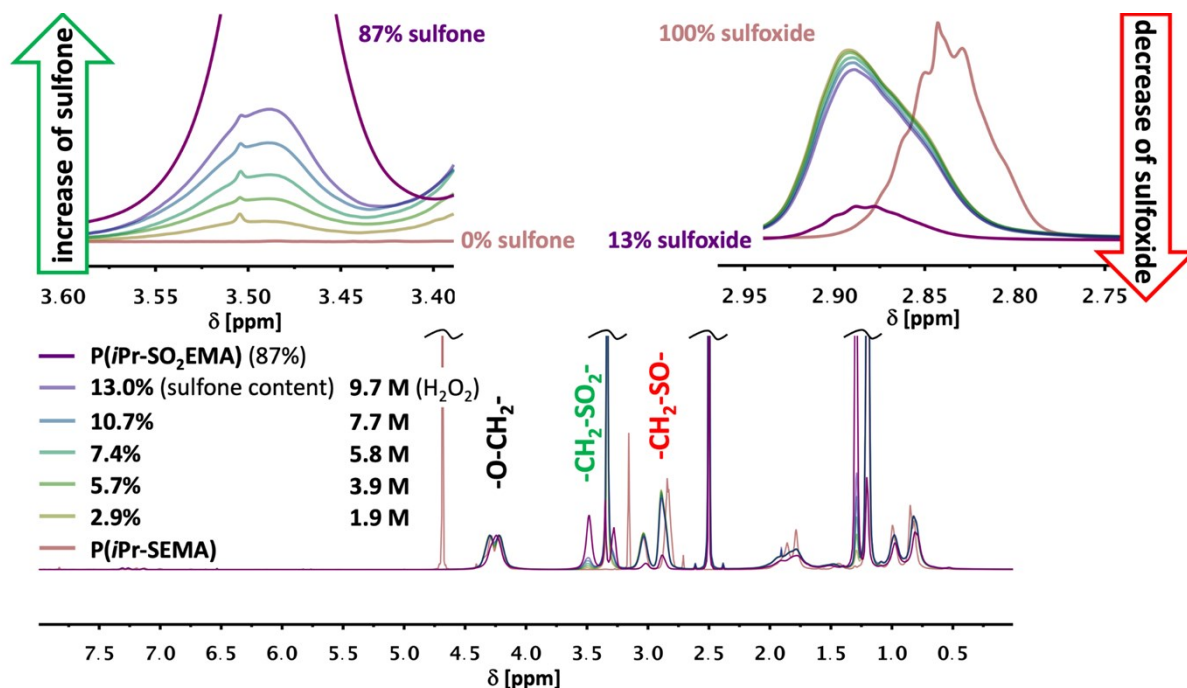
Fig. S12 ^{1}H-NMR investigation on the partial oxidation of P(iPr-SEMA)$_{128}$ after subjection to different H$_2$O$_2$ concentration (1.9 – 9.7 M) for 6 hours at 37 °C. Upon oxidation the aliphatic group next to the sulfoxide (-C**H**$_2$-SO-) at 2.89 ppm decreases gradually, while a new peak at 3.48 ppm appears which can be assigned to the sulfone (-C**H**$_2$-SO$_2$-). All spectra were normalized to the respective aliphatic group next to the methacrylate moiety (-O-C**H**$_2$-).

XI. Investigation of partially oxidized copolymer dispersions

The colloidal sizes of the partially oxidized P(nPr-SEMA) and P(iPr-SEMA) were determined in ultrapure water (c = 0.1 mg/mL) above their cloud point temperatures (50 °C for P(nPr-SEMA) and 80 °C for P(iPr-SEMA), respectively). The formed dispersions were investigated by dynamic light scattering (DLS) at a scattering angle of 90°C. By increasing the hydrophobic sulfone content in P(nPr-SEMA) from 3.2 mol% to 12.1 mol%, a gradual increase in size of the copolymer assemblies is observed (Fig. S13a-f). However, for the lowest (3.1 mol%, **Fig. S13a**) and highest (12.1%, **Fig. S13f**) sulfone content, the dispersions show broad particle distributions (441 ± 173 nm and 674 ± 241 nm, respectively). For an intermediate sulfone content of 7.9 mol% (**Fig. S13c**) the formed dispersion shows a narrower size distribution (921 ± 153 nm).

In contrast to P(nPr-SEMA), the partially oxidized P(iPr-SEMA) copolymers (**Fig. S13g-k**) do not show any clear trend with respect to their colloidal size. Although comparable sizes to P(nPr-SEMA) were observed, the resulting size distributions are much broader.

As a result, the DLS measurements suggest that for the P(nPr-SEMA) copolymers with an intermediate sulfone content (5.6-9.9 mol%) defined assemblies are formed while all P(iPr-SEMA) copolymers form undefined aggregates above the respective cloud point temperature.
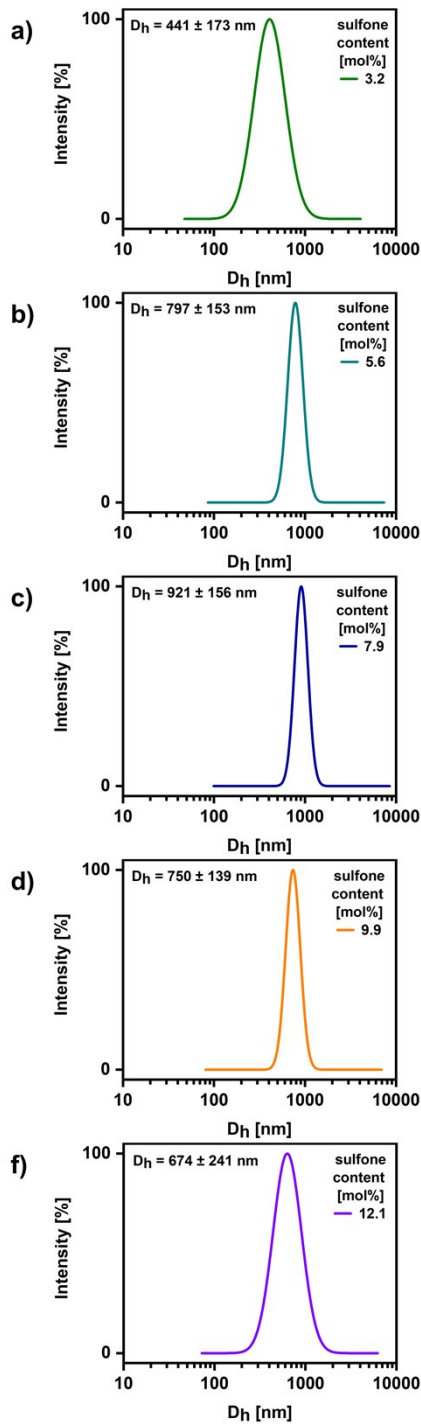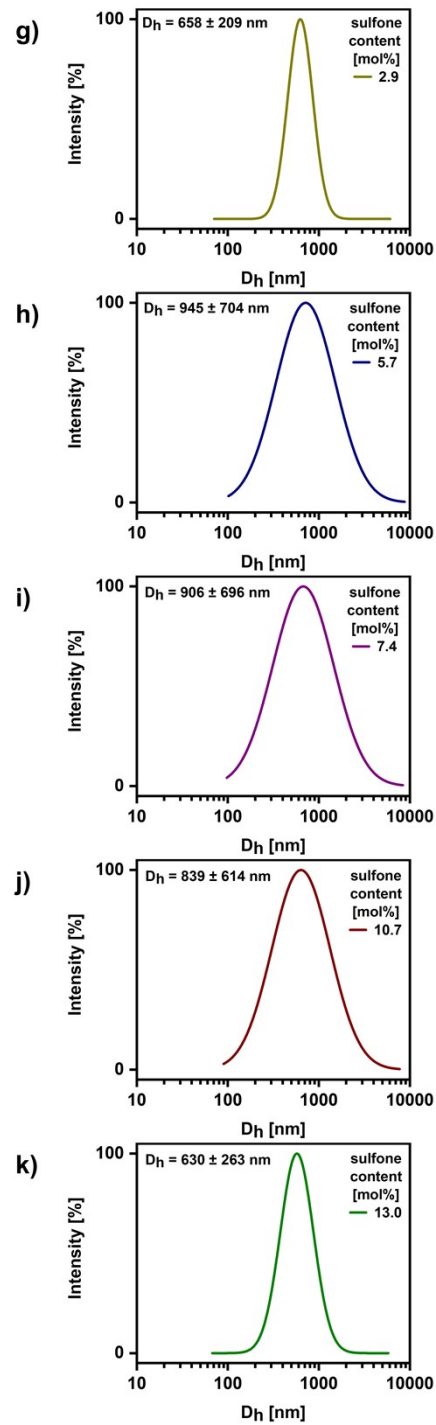
Fig. S13 Dynamic light scattering measurements on partially oxidized **(a-f)** P(*n*Pr-SEMA) and **(g-k)** P(*i*Pr-SEMA) amphiphilic copolymers above their cloud point temperatures at 50 °C for P(*n*Pr-SEMA) and 80 °C for P(*i*Pr-SEMA), respectively.

XII. Materials and syntheses

All starting materials and reagents were purchased from commercial sources and used without further purification, unless otherwise stated. Methacryloyl chloride (97%) and triethylamine (99%) were purchased from *abcr GmbH*. Anhydrous N,N-dimethylformamide (DMF, 99.8%, extra dry, stored over molecular sieve) was purchased from *Acros Organics*. 2-(methylthio)ethan-1-ol, 2-(ethylthio)ethan-1-ol, 2-(*i*-propylthio)ethan-1-ol, 2-(*n*-propylthio)ethan-1-ol, 2-(*n*-butylthio)ethan-1-ol and *p*-toluenesulfonic acid monohydrate were purchased from *Fluorochem Ltd.* Acryloyl chloride (stabilized with with phenothiazine) and α-methylstyrene (99%) were purchased from *Merck KGaA*. 2,2′-azobis(2-methylpropionitrile) (AIBN, 98%), carbon disulfide (≥99.9%), 2,6-di-*tert*-butyl-*p*-cresol (>99%), *meta*-chloroperbenzoic acid (*m*CPBA, ≥77%) and phenyl magnesium bromide solution (1M in THF) were purchased from *Sigma-Aldrich*. Cumyl dithiobenzoate (CDTB) was synthesized according to literature procedures.[5] Ultrapure water was taken from a LaboStar UV 2 water system. Moisture and/or air sensitive reactions were carried out in dry glassware under nitrogen atmosphere.

Synthesis of cumyl dithiobenzoate (CDTB)[5] Briefly, carbon disulfide (0.86 mL, 14.2 mmol) was added dropwise to an anhydrous solution of phenyl magnesium bromide (7.8 mL, 7.8 mmol, 1.0 M solution in THF) in 2.2 mL THF until the solution slightly boiled. After stirring for 1 hour at RT the reaction mixture was added to 50 g of ice and acidified with concentrated hydrochloric acid. The deep purple solution was then extracted with diethyl ether twice and dried in vacuo to yield 1.08 g (7.0 mmol, 89%) of a deep purple oil. The crude dithiobenzoic acid was used directly without further purification and added to α-methylstyrene (1.37 mL, 10.6 mmol) and *p*-toluenesulfonic acid (27 mg, 0.16 mmol) in 20 mL carbon tetrachloride. The reaction mixture was degassed by three consecutive freeze-pump-thaw cycles and refluxed under a nitrogen atmosphere overnight. The solvent was then removed in *vacuo* and the crude product was purified by column chromatography using *n*-hexane to yield 1.10 g (4.05 mmol, 58 %) of a deep purple solid. **CDTB** ^{1}H NMR (500 MHz, CDCl$_3$): δ = 7.86 (d, *J* = 7.4 Hz, 2H, *o*-ArH), 7.56 (d, *J* = 7.5 Hz, 2H, *o*-ArH), 7.47 (t, *J* = 7.4 Hz, 1H, *p*-ArH), 7.33 (td, *J* = 8.4, 1.7 Hz, 4H, *m*-ArH), 7.23 (t, *J* = 7.3 Hz, 1H, *p*-ArH), 2.02 (s, 6H, (-CH$_3$)$_2$) ppm. ^{13}C NMR (126 MHz, CDCl$_3$): δ = 227.27, 146.45, 144.35, 131.93, 128.27, 128.20, 126.90, 126.77, 126.76, 56.66, 28.44 ppm. HRMS: calc. for C$_{16}$H$_{16}$S$_2$ [M + Na]$^+$: 295.0591, found [M + Na]$^+$: 295.0563.

XIII. References

[1]   P. Vana, L. Albertin, L. Barner, T. P. Davis, C. Barner-Kowollik, *J. Polym. Sci., Part A: Polym. Chem.* **2002**, *40*, 4032-4037.

[2]   T. Gruendling, R. Pickford, M. Guilhaus, C. Barner-Kowollik, *J. Polym. Sci., Part A: Polym. Chem.* **2008**, *46*, 7447-7461.

[3]   H. Willcock, R. K. O'Reilly, *Polym. Chem.* **2010**, *1*, 149-157.

[4]   Q. Zhang, C. Weber, U. S. Schubert, R. Hoogenboom, *Mater. Horiz.* **2017**, *4*, 109-116.

[5]   H. Otsuka, T. Hagiwara, S. Yamamoto, *J. Nanosci. Nanotechnol.* **2014**, *14*, 6764-6773.